

Supplementary Materials for
Switchable oil-water phase separation of ionic liquids based
microemulsions by CO₂

Xiaoyan Pei, Dazhen Xiong, Yuanchao Pei, Huiyong Wang and Jianji Wang*

Collaborative Innovation Center of Henan Province for Green Manufacturing of Fine Chemicals, Henan Key Laboratory of Green Chemistry, Key Laboratory of Green Chemical Media and Reactions, Ministry of Education, School of Chemistry and Chemical Engineering, Henan Normal University, Xixiang, Henan 453007, P. R. China.

E-mail: Jwang@htu.cn

Table of Contents

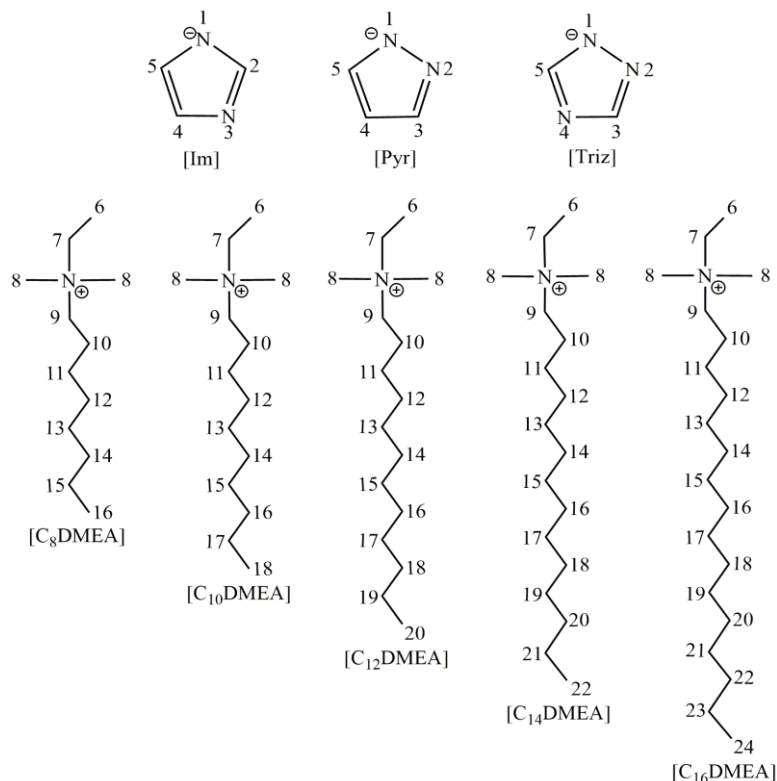
1. Experimental Section	S5
2. Tables S1-S2	
Table S1. The droplet size of n-pentanol/[C ₁₂ DMEA][Im]/H ₂ O microemulsions as a function of water content at 25 °C.	S10
Table S2. Yields for the reactions of aromatic aldehydes with malononitrile in [C ₁₂ DMEA][Im] based microemulsions.....	S10
3. Figures S1-S27	
Figure S1. Phase diagrams of the n-pentanol/[C _n DMEA][Pyr] (n = 8, 10, 12, 14, 16)/H ₂ O microemulsions (in mass fraction) at 25.0 °C.....	S11
Figure S2. Phase diagrams of the n-pentanol/[C _n DMEA][Triz] (n = 8, 10, 12, 14, 16)/H ₂ O microemulsions (in mass fraction) at 25.0 °C.....	S11
Figure S3. Phase diagrams of the n-pentanol/[C ₁₂ DMEA][Im]/H ₂ O (black), n-pentanol/[C ₁₂ DMEA][Pyr]/H ₂ O (red) and n-pentanol/[C ₁₂ DMEA][Triz]/H ₂ O microemulsions (blue) at 25.0 °C.....	S11
Figure S4. Electrical conductivity of the n-pentanol/[C ₁₂ DMEA][Im]/H ₂ O microemulsion as a function of water content (W_0) at different I values as stated at 25.0 °C.....	S12
Figure S5. Electrical conductivity of the n-pentanol/[C ₁₂ DMEA][Pyr]/H ₂ O microemulsion as a function of water content (W_0) at different I values as stated at 25.0 °C.....	S12
Figure S6. Phase diagram of the n-pentanol/[C ₁₂ DMEA][Pyr]/H ₂ O microemulsion at 25.0 °C with different types of microstructure; Circles (pink and blue) were results from DLS measurements.....	S13
Figure S7. Electrical conductivity of the n-pentanol/[C ₁₂ DMEA][Triz]/H ₂ O microemulsion as a function of water content (W_0) at different I values as stated at 25.0 °C.....	S13
Figure S8. Phase diagram of the n-pentanol/[C ₁₂ DMEA][Triz]/H ₂ O microemulsion with different types of microstructure at 25.0 °C; Circles (pink and blue) were results from DLS measurements.....	S14
Figure S9. SAXS curves of the n-pentanol/[C ₁₂ DMEA][Im]/H ₂ O microemulsion droplets at $I = 9.0$ (n-pentanol/[C ₁₂ DMEA][Im], 9:1, w/w) and different R values ($R =$	

H ₂ O/[C ₁₂ DMEA][Im] molar ratio) as stated.....	S14
Figure S10. Size distribution of the n-pentanol/[C ₁₂ DMEA][Im]/H ₂ O microemulsion droplets (n-pentanol/H ₂ O, 4 : 1, w/w) at different R (molar ratio of H ₂ O to [C ₁₂ DMEA][Im]) values.....	S14
Figure S11. Size distribution of the n-pentanol/[C ₁₂ DMEA][Pyr]/H ₂ O microemulsion droplets (n-pentanol/[C ₁₂ DMEA][Pyr], 11.3 : 1.0, w/w) and different R ₁ (molar ratio of H ₂ O to [C ₁₂ DMEA][Pyr]) values.....	S15
Figure S12. Size distributions of the n-pentanol/[C ₁₂ DMEA][Pyr]/H ₂ O microemulsion droplets (n-pentanol/H ₂ O, 4 : 1, w/w) at different R ₁ (molar ratio of H ₂ O to [C ₁₂ DMEA][Pyr]) values.....	S15
Figure S13. Linear correlation of size of the n-pentanol/[C _n DMEA][Pyr] (n= 8, 10, 12, 14, 16)/H ₂ O microemulsion droplets with the R ₁ values (molar ratio of H ₂ O to [C ₁₂ DMEA][Pyr]) at 25.0 °C.....	S15
Figure S14. Size distribution of the n-pentanol/[C ₁₂ DMEA][Triz]/H ₂ O microemulsion droplets (n-pentanol/[C ₁₂ DMEA][Triz], 8.8 : 1.0, w/w) and different R ₂ values (molar ratio of H ₂ O to [C ₁₂ DMEA][Triz]) values.....	S16
Figure S15. Size distribution of the n-pentanol/[C ₁₂ DMEA][Triz]/H ₂ O microemulsion droplets (n-pentanol/H ₂ O, 4 : 1, w/w) at different R ₂ values (molar ratio of H ₂ O to [C ₁₂ DMEA][Triz]).....	S16
Figure S16. Linear correlation of size of the n-pentanol/[C _n DMEA][Triz] (n= 8, 10, 12, 14, 16)/H ₂ O microemulsion droplets with the R ₂ values at 25.0 °C.....	S16
Figure S17. Linear change of absorbance intensity with concentrations of [C ₁₂ DMEA][Im]-CO ₂ in water at 206 nm.....	S17
Figure S18. ¹³ C NMR spectra of [C ₁₂ DMEA][Pyr] in the n-pentanol/[C ₁₂ DMEA][Pyr]/H ₂ O microemulsion system before bubbling of CO ₂ and after bubbling of N ₂ as well as in the aqueous solution after phase separation.....	S17
Figure S19. ¹³ C NMR of [C ₁₂ DMEA][Triz] in the n-pentanol/[C ₁₂ DMEA][Triz]/H ₂ O microemulsions system before bubbling of CO ₂ and after bubbling of N ₂ as well as in the aqueous solution after phase separation.....	S17
Figure S20. Change in size of the n-pentanol/[C ₁₂ DMEA][Im]/H ₂ O system with increasing	

concentrations of sodium bicarbonate.....	S18
Figure S21. ¹ H NMR spectrum of 2-benzylidenemalononitrile in CDCl ₃	S18
Figure S22. The reusability of [C ₁₂ DMEA][Im] based microemulsion in the reaction of benzaldehyde and malononitrile (1, 97.2%; 2, 96.2%; and 3, 94.5%).....	S18
Figure S23. ¹ H NMR spectrum of 3-(2,2-dicyanovinyl)phenyl nitrate in CDCl ₃	S19
Figure S24. ¹ H NMR spectrum of 4-(2,2-dicyanovinyl)phenyl nitrate in CDCl ₃	S19
Figure S25. ¹ H NMR spectrum of 2-(4-methylbenzylidene)malononitrile in CDCl ₃	S19
Figure S26. ¹ H NMR spectrum of 2-(4-fluorobenzylidene)malononitrile in CDCl ₃	S20
Figure S27. ¹ H NMR spectrum of 2-(furan-2-ylmethylene)malononitrile in CDCl ₃	S20
References	S20

Experimental Section

1. NMR and IR data of the ILs



Numbering of the position of carbon atoms in the anions and cations of the ILs

[C₈DMEA][Im]: ¹H NMR (D₂O, TMS): δ 0.75 (t, 3H, CH₃), 1.24 (m, 13H, CH₂ and CH₃), 1.62 (m, 2H, CH₂), 2.89 (s, 6H, CH₃), 3.11 (t, 2H, CH₂), 3.24 (m, 2H, CH₂), 7.02 (s, 2H, Im C4 and C5), 7.64 (s, 1H, Im C2) ppm; ¹³C NMR (D₂O, TMS): δ 7.35 (C6), 13.47 (C16), 21.69 (C15), 22.01 (C10), 25.48 (C11), 28.18 (C12), 28.22 (C13), 31.02 (C14), 49.75 (C8), 49.80 (C8), 59.32 (C7), 63.36 (C9), 122.50 (C4), 122.55 (C5), 137.69 (C2) ppm; IR: ν 3070, 2955, 2925, 2856, 1707, 1634, 1446, 1378, 1289, 1215, 1150, 1076, 1022, 979, 920, 820, 757, 724 cm⁻¹.

[C₁₀DMEA][Im]: ¹H NMR (D₂O, TMS): δ 0.76 (t, 3H, CH₃), 1.19 (m, 17H, CH₂ and CH₃), 1.63 (m, 2H, CH₂), 2.91 (s, 6H, CH₃), 3.12 (t, 2H, CH₂), 3.25 (m, 2H, CH₂), 7.03 (s, 2H, Im C4 and C5), 7.66 (s, 1H, Im C2) ppm; ¹³C NMR (D₂O, TMS): δ 7.39 (C6), 13.77 (C18), 21.90 (C17), 22.43 (C10), 25.80 (C11), 28.68 (C12), 29.03 (C15), 29.09 (C13), 29.18 (C14), 31.65 (C16), 49.85 (C8), 49.85 (C8), 59.24 (C7), 63.11 (C9), 122.49 (C4), 122.54 (C5), 137.96 (C2) ppm; IR: ν 3152, 2923, 2854, 1577, 1467, 1381, 1323, 1024, 900, 870, 817, 721 cm⁻¹.

[C₁₂DMEA][Im]: ¹H NMR (D₂O, TMS): δ 0.81 (t, 3H, CH₃), 1.21 (m, 21H, CH₂ and CH₃), 1.48 (m, 2H, CH₂), 2.79 (m, 6H, CH₃), 2.94 (t, 2H, CH₂), 3.11 (m, 2H, CH₂), 6.93 (s, 2H, Im C4 and C5), 7.57 (s, 1H, Im C2) ppm; ¹³C NMR (D₂O, TMS): δ 7.39 (C6), 13.88 (C20), 22.00 (C19), 22.62 (C10), 25.99 (C11), 28.98 (C12), 29.40 (C17), 29.45 (C13), 29.58 (C14), 29.70 (C15), 29.73 (C16), 31.92 (C18), 48.83 (C8), 48.83 (C8), 59.14 (C7), 62.93 (C9), 122.53 (C4 and C5), 138.11 (C2) ppm; IR: ν 3100, 2923, 2854, 1635, 1579, 1467, 1381, 1323, 1294, 1248, 1092, 1024, 977, 909, 818, 743 cm⁻¹.

[C₁₄DMEA][Im]: ¹H NMR (D₂O, TMS): δ 0.81 (t, 3H, CH₃), 1.23 (m, 25H, CH₂ and CH₃), 1.51 (m, 2H, CH₂), 2.83 (s, 6H, CH₃), 2.97 (t, 2H, CH₂), 3.13 (m, 2H, CH₂), 6.96 (s, 2H, Im C4 and C5), 7.60 (s, 1H, Im C2) ppm; ¹³C NMR (D₂O, TMS): δ 7.42 (C6), 13.88 (C22), 22.01 (C21), 22.63 (C10), 26.00 (C11), 28.99 (C12), 28.99 (C19), 29.41 (C13), 29.45 (C14), 29.59 (C15), 29.70 (C16), 29.74 (C17), 29.74 (C18), 31.93 (C20), 49.84 (C8), 49.84 (C8), 59.15 (C7), 62.94 (C9), 122.90 (C4 and C5), 139.01 (C2) ppm; IR: ν 3106, 2923, 2853, 1578, 1467, 1385, 1323, 1248, 1141, 1092, 1022, 910, 819, 744, 722 cm⁻¹.

[C₁₆DMEA][Im]: ¹H NMR (D₂O, TMS): δ 0.81 (t, 3H, CH₃), 1.22 (m, 29H, CH₂ and CH₃), 1.62 (m, 2H, CH₂), 2.96 (s, 6H, CH₃), 3.13 (m, 2H, CH₂), 3.28 (m, 2H, CH₂), 7.03 (s, 2H, Im C4 and C5), 7.68 (s, 1H, Im C2) ppm; ¹³C NMR (D₂O, TMS): δ 7.42 (C6), 13.82 (C24), 22.04 (C23), 22.61 (C10), 26.02 (C11), 29.05 (C12), 29.05 (C21), 29.46 (C13), 29.54 (C14), 29.70 (C15), 29.70 (C16), 29.79 (C17), 29.79 (C18), 29.89 (C19), 29.92 (C20), 31.94 (C22), 50.06 (C8), 50.06 (C8), 59.09 (C7), 62.75 (C9), 121.54 (C4 and C5), 136.02 (C2) ppm; IR: ν 3080, 2918, 2851, 1633, 1468, 1379, 1338, 1295, 1151, 1076, 1023, 979, 924, 836, 759, 720 cm⁻¹.

[C₈DMEA][Pyr]: ¹H NMR (D₂O, TMS): δ 0.77 (t, 3H, CH₃), 1.22 (m, 13H, CH₂ and CH₃), 1.62 (m, 2H, CH₂), 2.90 (s, 6H, CH₃), 3.13 (t, 2H, CH₂), 3.22 (m, 2H, CH₂), 6.32 (s, 1H, Pyr C4), 7.57 (s, 2H, Pyr C3 and C5) ppm; ¹³C NMR (D₂O, TMS): δ 7.34 (C6), 13.66 (C16), 21.75 (C15), 22.24 (C10), 25.63 (C11), 28.44 (C12), 28.54 (C13), 31.29 (C14), 49.76 (C8), 49.76 (C8), 59.30 (C7), 63.07 (C9), 104.03 (C4), 134.88 (C3 and C5) ppm; IR: ν 3022, 2925, 2856, 1636, 1462, 1349, 1281, 1208,

1141, 1065, 1008, 980, 916, 841, 736 cm^{-1} .

[C₁₀DMEA][Pyr]: ¹H NMR (D₂O, TMS): δ 0.77 (t, 3H, CH₃), 1.19 (m, 17H, CH₂ and CH₃), 1.61 (m, 2H, CH₂), 2.89 (s, 6H, CH₃), 3.11 (t, 2H, CH₂), 3.23 (m, 2H, CH₂), 6.31 (s, 1H, Pyr C4), 7.61 (s, 2H, Pyr C3 and C5) ppm; ¹³C NMR (D₂O, TMS): δ 7.38 (C6), 13.85 (C18), 21.89 (C17), 22.55 (C10), 25.87 (C11), 28.83 (C12), 29.22 (C15), 29.28 (C13), 29.36 (C14), 31.81 (C16), 49.82 (C8), 49.82 (C8), 59.14 (C7), 62.87 (C9), 103.70 (C4), 134.89 (C3 and C5) ppm; IR: ν 3050, 2923, 2854, 1714, 1636, 1464, 1378, 1350, 1281, 1213, 1143, 1011, 916, 842, 812, 736 cm^{-1} .

[C₁₂DMEA][Pyr]: ¹H NMR (D₂O, TMS): δ 0.84 (t, 3H, CH₃), 1.24 (m, 21H, CH₂ and CH₃), 1.44 (m, 2H, CH₂), 2.80 (s, 6H, CH₃), 2.89 (t, 2H, CH₂), 3.10 (m, 2H, CH₂), 6.18 (m, 1H, Pyr C4), 7.53 (d, 2H, Pyr C3 and C5) ppm; ¹³C NMR (D₂O, TMS): δ 7.41 (C6), 13.88 (C20), 21.99 (C19), 22.63 (C10), 25.99 (C11), 28.98 (C12), 29.41 (C17), 29.45 (C13), 29.58 (C14), 29.70 (C15), 29.74 (C16), 31.93 (C18), 49.85 (C8), 49.85 (C8), 59.14 (C7), 62.90 (C9), 103.72 (C4), 138.16 (C3 and C5) ppm; IR: ν 3032, 2923, 2853, 1635, 1465, 1378, 1351, 1280, 1213, 1143, 1014, 917, 842, 812, 738 cm^{-1} .

[C₁₄DMEA][Pyr]: ¹H NMR (D₂O, TMS): δ 0.84 (t, 3H, CH₃), 1.24 (m, 25H, CH₂ and CH₃), 1.46 (m, 2H, CH₂), 2.81 (s, 6H, CH₃), 2.91 (t, 2H, CH₂), 3.10 (m, 2H, CH₂), 6.21 (m, 1H, Pyr C4), 7.55 (m, 2H, Pyr C3 and C5) ppm; ¹³C NMR (D₂O, TMS): δ 7.42 (C6), 13.89 (C22), 21.96 (C21), 22.65 (C10), 25.99 (C11), 29.01 (C12), 29.01 (C19), 29.46 (C13), 29.50 (C14), 29.63 (C15), 29.63 (C16), 29.75 (C17), 29.79 (C18), 31.97 (C20), 49.87 (C8), 49.87 (C8), 59.11 (C7), 62.77 (C9), 103.53 (C4), 134.80 (C3 and C5) ppm; IR: ν 3070, 2922, 2853, 1640, 1465, 1394, 1351, 1308, 1282, 1216, 1144, 1014, 918, 844, 737 cm^{-1} .

[C₁₆DMEA][Pyr]: ¹H NMR (D₂O, TMS): δ 0.82 (t, 3H, CH₃), 1.22 (m, 29H, CH₂ and CH₃), 1.53 (m, 2H, CH₂), 2.91 (s, 6H, CH₃), 3.04 (t, 2H, CH₂), 3.20 (m, 2H, CH₂), 6.26 (m, 1H, Pyr C4), 7.58 (m, 2H, Pyr C3 and C5) ppm; ¹³C NMR (D₂O, TMS): δ 7.41 (C6), 13.83 (C24), 22.00 (C23), 22.63 (C10), 25.98 (C11), 29.04 (C12), 29.04 (C21), 29.49 (C13), 29.49 (C14), 29.54 (C15), 29.54 (C16), 29.71 (C17), 29.71 (C18), 29.82 (C19), 29.95 (C20), 31.97 (C22), 50.04 (C8), 50.04 (C8), 59.08 (C7), 62.72

(C9), 104.49 (C4), 133.88 (C3 and C5) ppm; IR: ν 3020, 2917, 2850, 1632, 1468, 1377, 1281, 1143, 1007, 990, 927, 889, 838, 752 cm^{-1} .

[C₈DMEA][Triz]: ¹H NMR (D₂O, TMS): δ 0.77 (t, 3H, CH₃), 1.20 (m, 13H, CH₂ and CH₃), 1.60 (m, 2H, CH₂), 2.87 (s, 6H, CH₃), 3.10 (t, 2H, CH₂), 3.22 (m, 2H, CH₂), 8.03 (s, 2H, Triz C3 and C5) ppm; ¹³C NMR (D₂O, TMS): δ 7.34 (C6), 13.56 (C16), 21.71 (C15), 22.10 (C10), 25.53 (C11), 28.26 (C12), 28.32 (C13), 31.11 (C14), 49.74 (C8), 49.74 (C8), 59.29 (C7), 63.33 (C9), 149.61 (C3 and C5) ppm; IR: ν 3073, 2925, 2857, 1644, 1470, 1378, 1240, 1183, 1142, 1020, 962, 926, 849, 814, 723, 683 cm^{-1} .

[C₁₀DMEA][Triz]: ¹H NMR (D₂O, TMS): δ 0.79 (t, 3H, CH₃), 1.20 (m, 17H, CH₂ and CH₃), 1.58 (m, 2H, CH₂), 2.86 (s, 6H, CH₃), 3.07 (t, 2H, CH₂), 3.20 (m, 2H, CH₂), 8.02 (s, 2H, Triz C3 and C5) ppm; ¹³C NMR (D₂O, TMS): δ 7.38 (C6), 13.82 (C18), 21.91 (C17), 22.49 (C10), 25.84 (C11), 28.75 (C12), 29.12 (C15), 29.17 (C13), 29.26 (C14), 31.72 (C16), 49.82 (C8), 49.82 (C8), 59.25 (C7), 63.12 (C9), 149.56 (C3 and C5) ppm; IR: ν 3053, 2920, 2837, 1643, 1455, 1387, 1220, 1153, 1112, 1020, 972, 936, 849, 804, 723, 683 cm^{-1} .

[C₁₂DMEA][Triz]: ¹H NMR (D₂O, TMS): δ 0.83 (t, 3H, CH₃), 1.24 (m, 21H, CH₂ and CH₃), 1.52 (m, 2H, CH₂), 2.82 (s, 6H, CH₃), 2.99 (t, 2H, CH₂), 3.15 (m, 2H, CH₂), 8.00 (s, 2H, Triz C3 and C5) ppm; ¹³C NMR (D₂O, TMS): δ 7.41 (C6), 13.87 (C20), 22.01 (C19), 23.42 (C10), 26.00 (C11), 28.99 (C12), 29.41 (C17), 29.46 (C13), 29.59 (C14), 29.70 (C15), 29.74 (C16), 31.92 (C18), 49.87 (C8), 49.87 (C8), 59.21 (C7), 63.01 (C9), 148.76 (C3 and C5) ppm; IR: ν 3025, 2923, 2854, 1582, 1470, 1380, 1271, 1242, 1143, 1063, 1022, 962, 928, 854, 814, 722, 683 cm^{-1} .

[C₁₄DMEA][Triz]: ¹H NMR (D₂O, TMS): δ 0.82 (t, 3H, CH₃), 1.23 (m, 25H, CH₂ and CH₃), 1.55 (m, 2H, CH₂), 2.84 (s, 6H, CH₃), 3.02 (t, 2H, CH₂), 3.18 (m, 2H, CH₂), 8.00 (s, 2H, Triz C3 and C5) ppm; ¹³C NMR (D₂O, TMS): δ 7.34 (C6), 13.87 (C22), 21.95 (C21), 22.63 (C10), 25.97 (C11), 29.01 (C12), 29.01 (C19), 29.48 (C13), 29.52 (C14), 29.68 (C15), 29.80 (C16), 29.89 (C17), 29.89 (C18), 31.96 (C20), 49.77 (C8), 49.77 (C8), 59.07 (C7), 62.87 (C9), 149.78 (C3 and C5) ppm; IR: ν 3050, 2923, 2854, 1583, 1469, 1379, 1270, 1240, 1184, 1142, 1022, 962, 928, 851, 814, 721, 684 cm^{-1} .

[C₁₆DMEA][Triz]: ¹H NMR (D₂O, TMS): δ 0.77 (t, 3H, CH₃), 1.18 (m, 29H, CH₂

and CH₃), 1.36 (m, 2H, CH₂), 2.68 (s, 6H, CH₃), 2.81 (t, 2H, CH₂), 2.98 (m, 2H, CH₂), 7.88 (s, 2H, Triz C3 and C5) ppm; ¹³C NMR (D₂O, TMS): δ 7.37 (C6), 13.88 (C24), 21.97 (C23), 22.66 (C10), 26.00 (C11), 29.07 (C12), 29.07 (C21), 29.54 (C13), 29.54 (C20), 29.59 (C14), 29.59 (C19), 29.76 (C15), 29.76 (C18), 29.87 (C16), 30.01 (C17), 32.00 (C22), 49.79 (C8), 49.79 (C8), 59.06 (C7), 62.83 (C9), 149.57 (C3 and C5) ppm; IR: ν 3020, 2917, 2850, 1629, 1470, 1375, 1337, 1235, 1186, 1140, 1024, 971, 930, 838, 719, 684 cm⁻¹.

2. Determination of bromide content in the ILs.

Bromide contents in the ILs were determined by means of a Br⁻ selective electrode (Shanghai Precision & Scientific Instrument Co. Ltd) coupled with a 6802 saturated calomel electrode, and a PHSJ-4F digital pH meter was used to measure the potentials. The measurements were conducted at 25 ± 0.1 °C, and calibration curves were obtained from the potential values against concentrations of aqueous solutions of the corresponding precursor bromide ionic liquids. Each experiment was performed in triplicate, and the reproducibility was within 2%.

3. Analysis of the composition of the aqueous phase after phase separation.

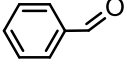
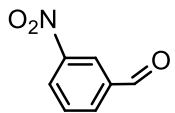
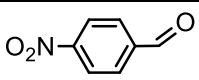
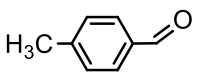
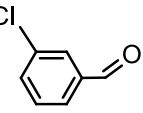
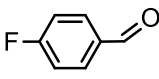
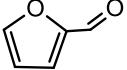
The concentration of the residual ILs in the aqueous solution after phase separation was determined by spectrophotometric method.^[1-3] Briefly, we prepared a given concentration of aqueous IL solutions saturated with CO₂ at 25 °C as mother-liquid of sample firstly. Then, a series of different concentrations of the ILs-CO₂ aqueous solutions were obtained by diluting the above sample solution under an atmosphere of carbon dioxide. The absorbance of each of them was measured in a 1 cm cell, and then standard curve was established through fitting the absorbance intensity with different concentrations of IL. Taking [C₁₂DMEA][Im] as an example, a series of standard solutions of the IL reacted with CO₂ were prepared and their absorbance intensity was measured at 206 nm, respectively. The absorbance intensity of [C₁₂DMEA][Im] was obtained as a linear function of the IL content in water (Figure S16). Thus, the content of the residual [C₁₂DMEA][Im] in the aqueous solution after phase separation could be read from the standard curve by measuring its corresponding absorbance intensity.

Tables S1-S2

Table S1. The droplet size of n-pentanol/[C₁₂DMEA][Im]/H₂O microemulsions as a function of water content at 25 °C.

microemulsion	R	Size distribution (nm)	Mean (nm)	PDI	Number (%)
n-pentanol/[C ₁₂ DMEA][Im]/H ₂ O	9.28	1.5 ~ 2.7	2.0	0.209	100
	19.30	4.2 ~ 8.7	5.6	0.176	100
	31.38	6.5 ~ 15.7	8.7	0.151	100
	43.26	7.5 ~ 15.7	10.1	0.124	100
	57.01	7.9 ~ 28.2	15.7	0.222	100

Table S2. Yields for the reactions of aromatic aldehydes with malononitrile in [C₁₂DMEA][Im] based microemulsions.

Entry	R ^a	Yield (%) ^b
1		97.2
2		93.2
3		98.3
4		94.5
5		95.0
6		96.2
7		98.7

[a] All of these reactions were performed with aldehyde (1.05 mmol) and malononitrile (1.00 mmol) in 1.5 mL of microemulsion at 25 °C for 1h.

[b] Determined by ¹H NMR using anisole as an internal standard.

Figures S1-S27

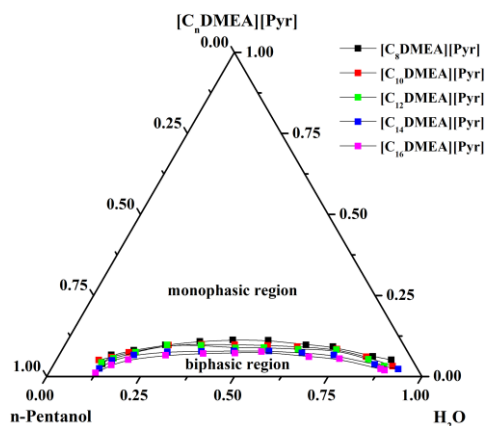


Figure S1. Phase diagrams of the n-pentanol/[C_nDMEA][Pyr] (n = 8, 10, 12, 14, 16)/H₂O microemulsions (in mass fraction) at 25.0 °C.

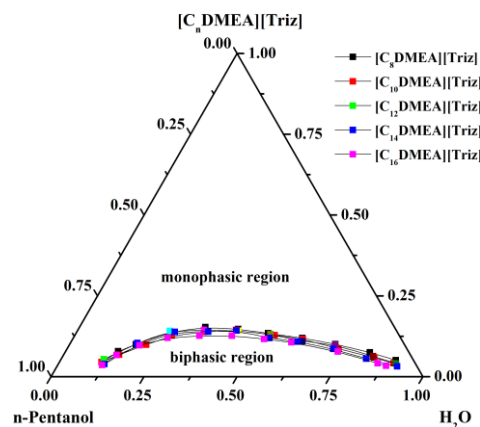


Figure S2. Phase diagrams of the n-pentanol/[C_nDMEA][Triz] (n = 8, 10, 12, 14, 16)/H₂O microemulsions (in mass fraction) at 25.0 °C.

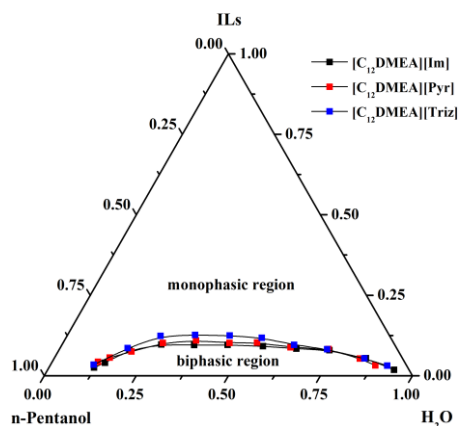


Figure S3. Phase diagrams of the n-pentanol/[C₁₂DMEA][Im]/H₂O (black), n-pentanol/[C₁₂DMEA][Pyr]/H₂O (red) and n-pentanol/[C₁₂DMEA][Triz]/H₂O microemulsions (blue) at 25.0 °C.

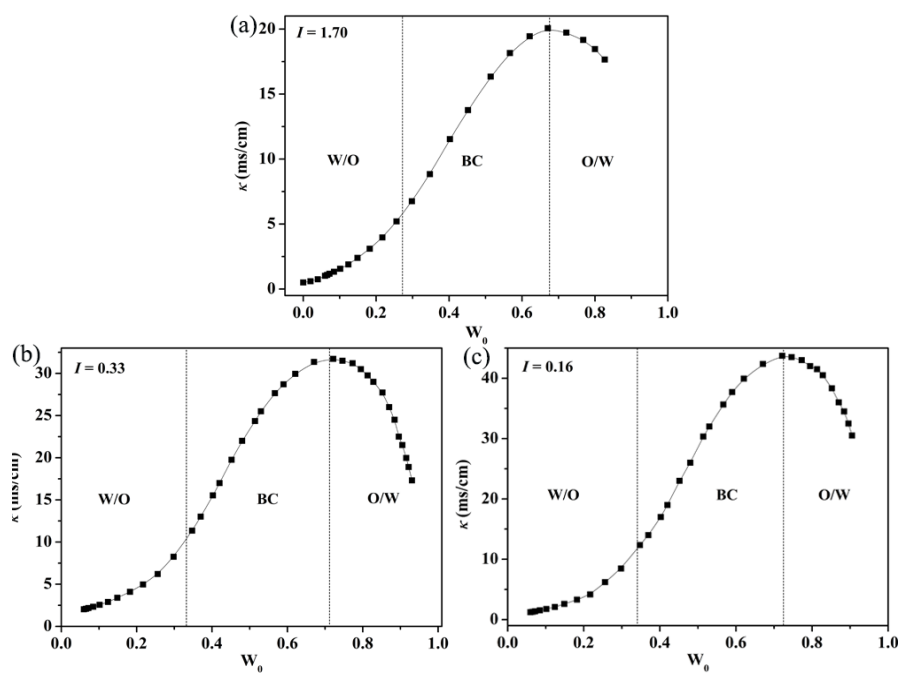


Figure S4. Electrical conductivity of the n-pentanol/[C₁₂DMEA][Im]/H₂O microemulsion as a function of water content (W_0) at different I values as stated at 25.0 °C.

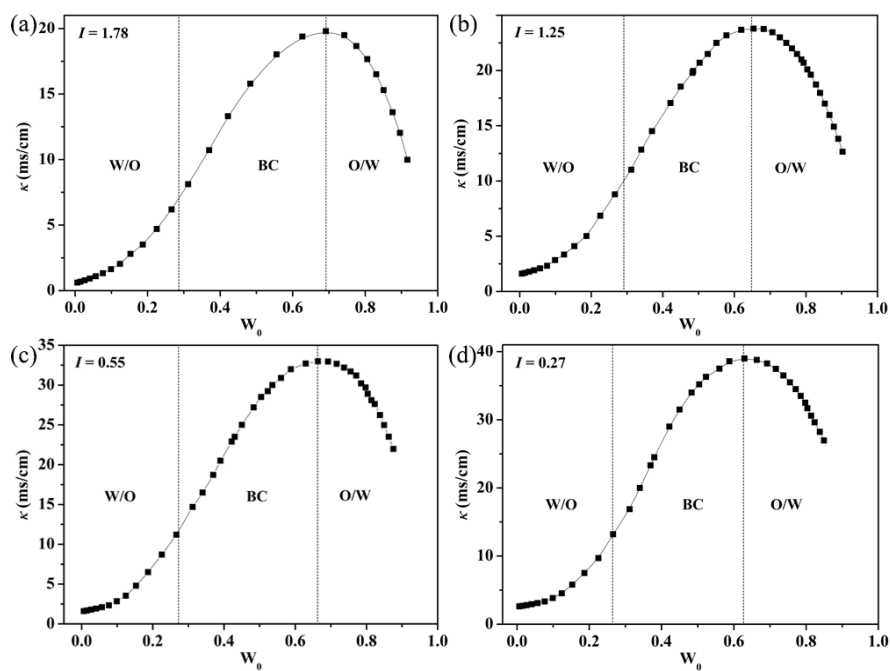


Figure S5. Electrical conductivity of the n-pentanol/[C₁₂DMEA][Pyr]/H₂O microemulsion as a function of water content (W_0) at different I values as stated at 25.0 °C.

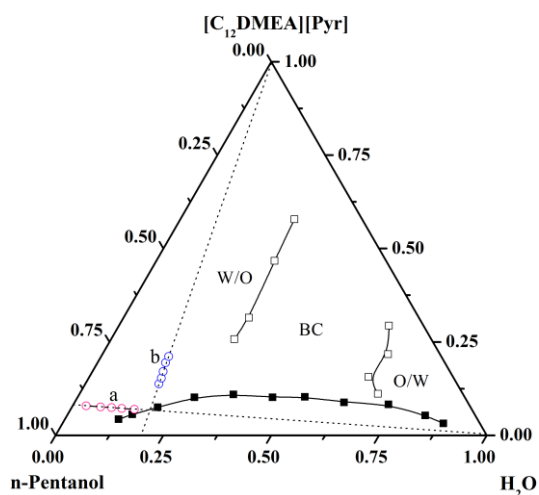


Figure S6. Phase diagram of the n-pentanol/[C₁₂DMEA][Pyr]/H₂O microemulsion at 25.0 °C with different types of microstructure; Circles (pink and blue) were results from DLS measurements.

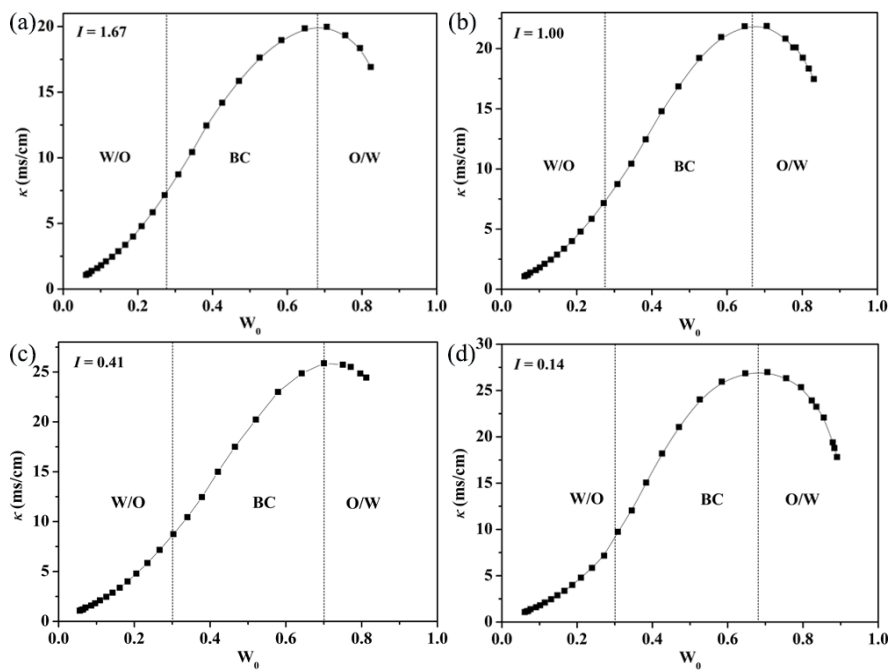


Figure S7. Electrical conductivity of the n-pentanol/[C₁₂DMEA][Triz]/H₂O microemulsion as a function of water content (W_0) at different I values as stated at 25.0 °C.

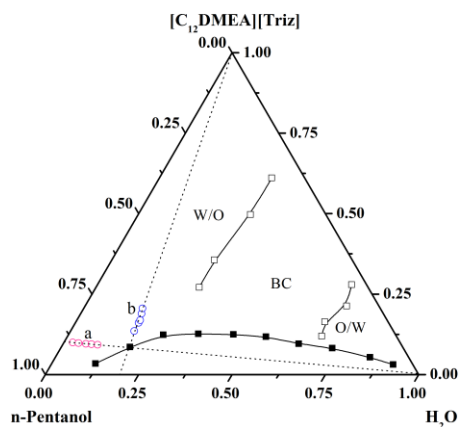


Figure S8. Phase diagram of the n-pentanol/[C₁₂DMEA][Triz]/H₂O microemulsion with different types of microstructure at 25.0 °C; Circles (pink and blue) were results from DLS measurements.

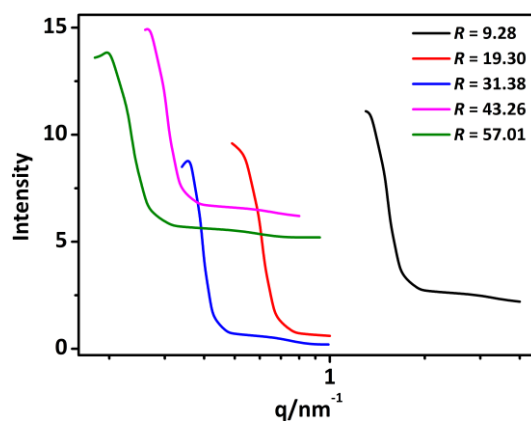


Figure S9. SAXS curves of the n-pentanol/[C₁₂DMEA][Im]/H₂O microemulsion droplets at $I = 9.0$ (n-pentanol/[C₁₂DMEA][Im], 9:1, w/w) and different R values ($R = \text{H}_2\text{O}/[\text{C}_{12}\text{DMEA}][\text{Im}]$ molar ratio) as stated.

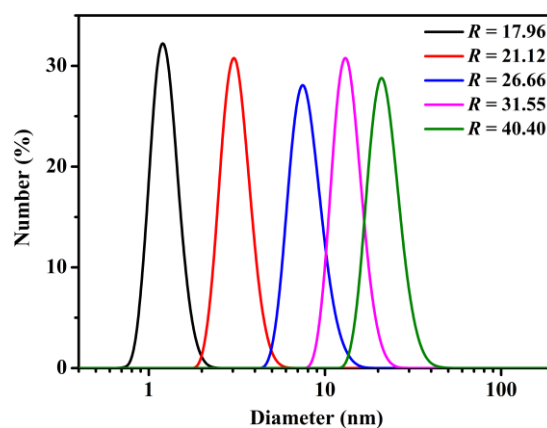


Figure S10. Size distribution of the n-pentanol/[C₁₂DMEA][Im]/H₂O microemulsion droplets (n-pentanol/H₂O, 4 : 1, w/w) at different R (molar ratio of H₂O to [C₁₂DMEA][Im]) values.

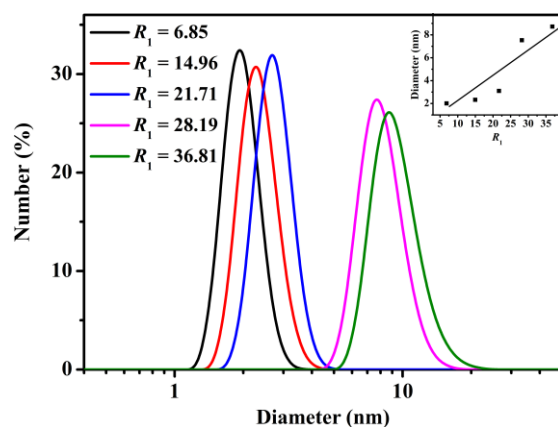


Figure S11. Size distribution of the n-pentanol/[C₁₂DMEA][Pyr]/H₂O microemulsion droplets (n-pentanol/[C₁₂DMEA][Pyr], 11.3 : 1.0, w/w) and different R_1 (molar ratio of H₂O to [C₁₂DMEA][Pyr]) values.

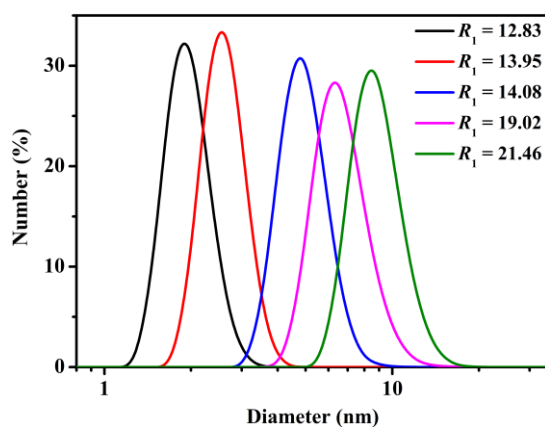


Figure S12. Size distributions of the n-pentanol/[C₁₂DMEA][Pyr]/H₂O microemulsion droplets (n-pentanol/H₂O, 4 : 1, w/w) at different R_1 (molar ratio of H₂O to [C₁₂DMEA][Pyr]) values.

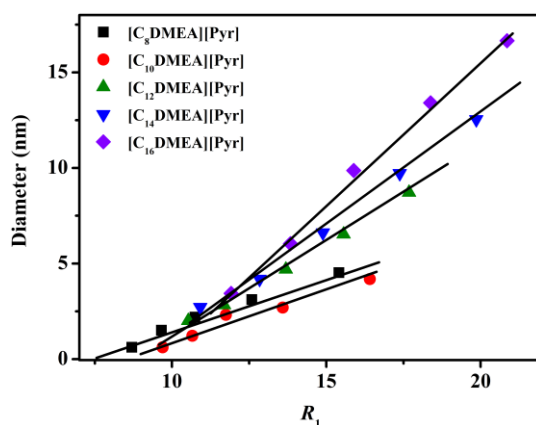


Figure S13. Linear correlation of size of the n-pentanol/[C_nDMEA][Pyr] (n= 8, 10, 12, 14, 16)/H₂O microemulsion droplets with the R_1 values (molar ratio of H₂O to [C₁₂DMEA][Pyr]) at 25.0 °C.

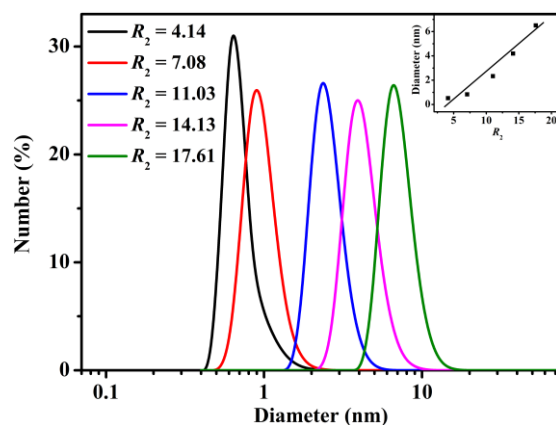


Figure S14. Size distribution of the n-pentanol/[C₁₂DMEA][Triz]/H₂O microemulsion droplets (n-pentanol/[C₁₂DMEA][Triz], 8.8 : 1.0, w/w) and different R_2 values (molar ratio of H₂O to [C₁₂DMEA][Triz]) values.

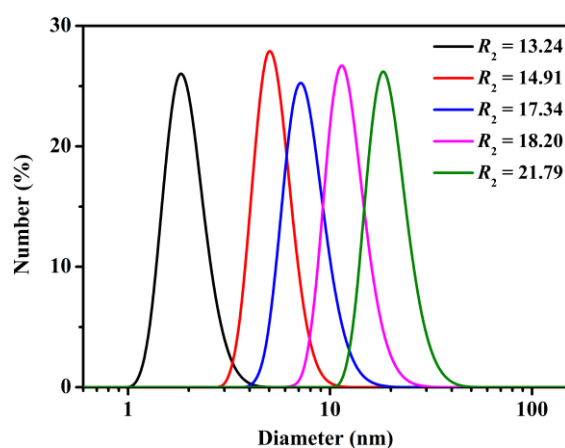


Figure S15. Size distribution of the n-pentanol/[C₁₂DMEA][Triz]/H₂O microemulsion droplets (n-pentanol/H₂O, 4 : 1, w/w) at different R_2 values (molar ratio of H₂O to [C₁₂DMEA][Triz]).

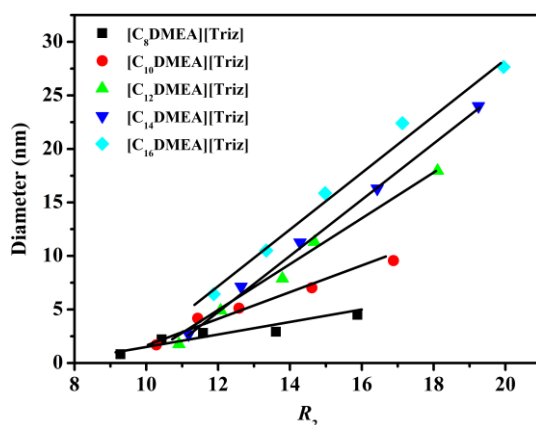


Figure S16. Linear correlation of size of the n-pentanol/[C_nDMEA][Triz] (n = 8, 10, 12, 14, 16)/H₂O microemulsion droplets with the R_2 values at 25.0 °C.

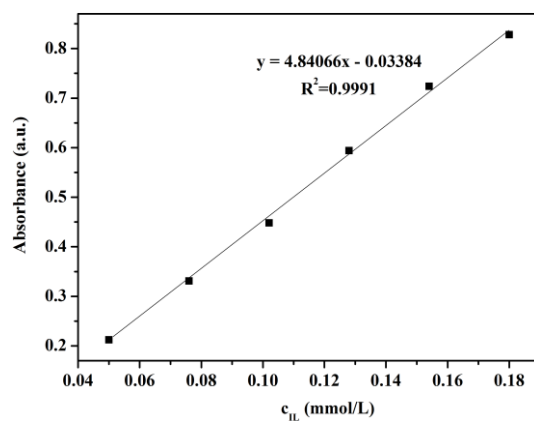


Figure S17. Linear change of absorbance intensity with concentrations of $[C_{12}DMEA][Im]-CO_2$ in water at 206 nm.

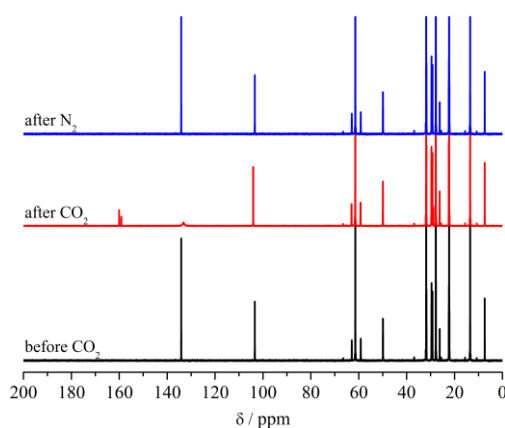


Figure S18. ^{13}C NMR spectra of $[C_{12}DMEA][Pyr]$ in the n-pentanol/ $[C_{12}DMEA][Pyr]/H_2O$ microemulsion system before bubbling of CO_2 and after bubbling of N_2 as well as in the aqueous solution after phase separation.

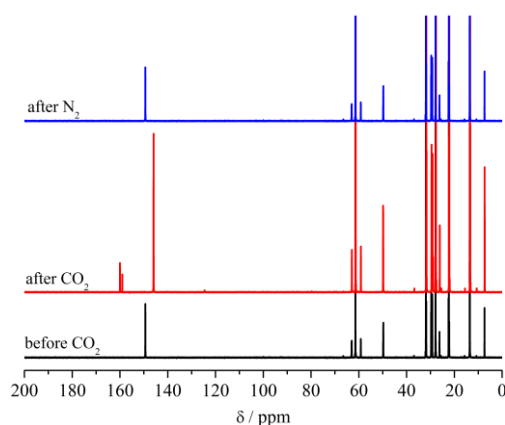


Figure S19. ^{13}C NMR of $[C_{12}DMEA][Triz]$ in the n-pentanol/ $[C_{12}DMEA][Triz]/H_2O$ microemulsions system before bubbling of CO_2 and after bubbling of N_2 as well as in the aqueous solution after phase separation.

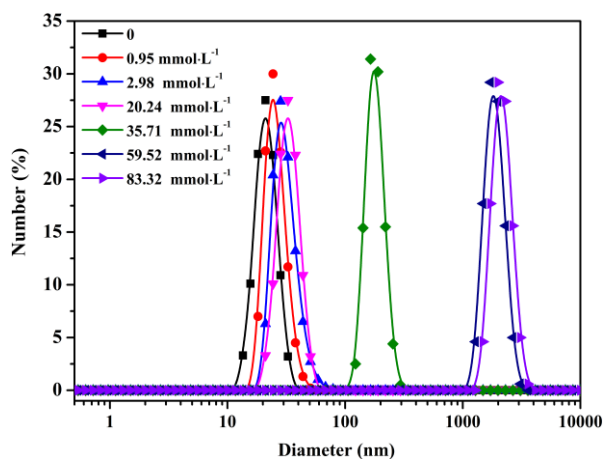


Figure S20. Change in size of the n-pentanol/[C₁₂DMEA][Im]/H₂O system with increasing concentrations of sodium bicarbonate.

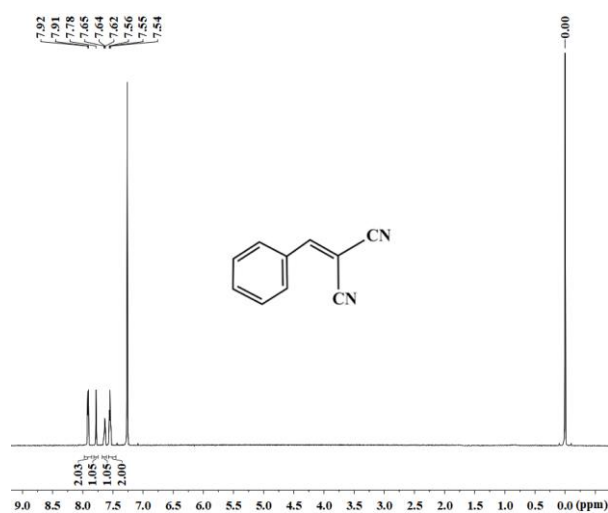


Figure S21. ¹H NMR spectrum of 2-benzylidenemalononitrile in CDCl₃.

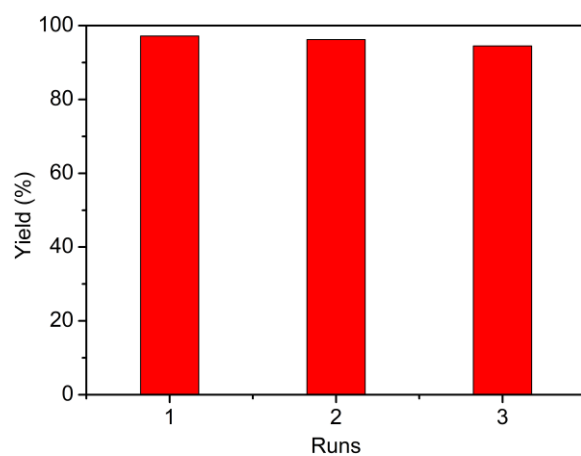


Figure S22. The reusability of [C₁₂DMEA][Im] based microemulsion in the reaction of benzaldehyde and malononitrile (1, 97.2%; 2, 96.2%; and 3, 94.5%).

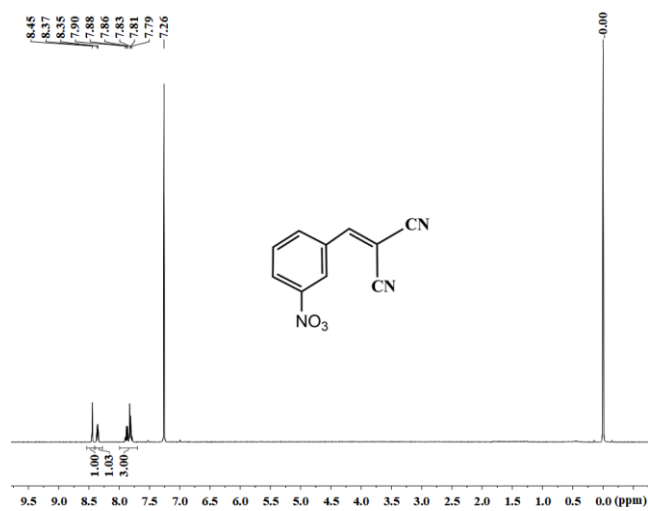


Figure S23. ^1H NMR spectrum of 3-(2,2-dicyanovinyl)phenyl nitrate in CDCl_3 .

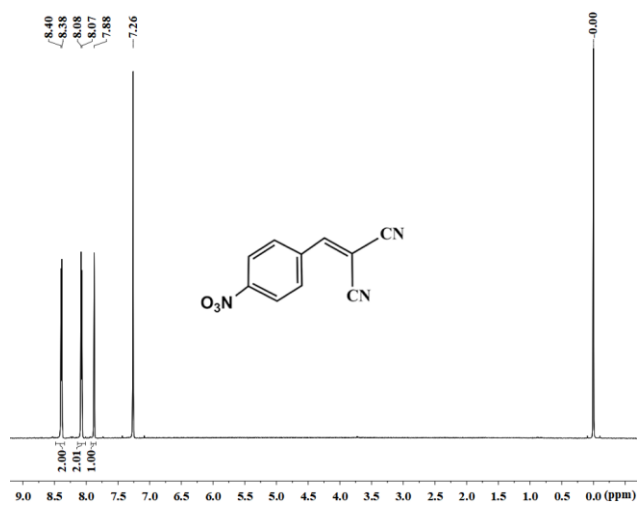


Figure S24. ^1H NMR spectrum of 4-(2,2-dicyanovinyl)phenyl nitrate in CDCl_3 .

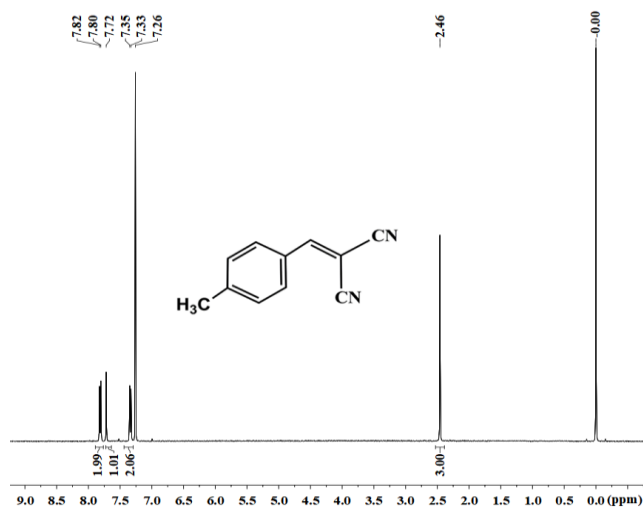


Figure S25. ^1H NMR spectrum of 2-(4-methylbenzylidene)malononitrile in CDCl_3 .

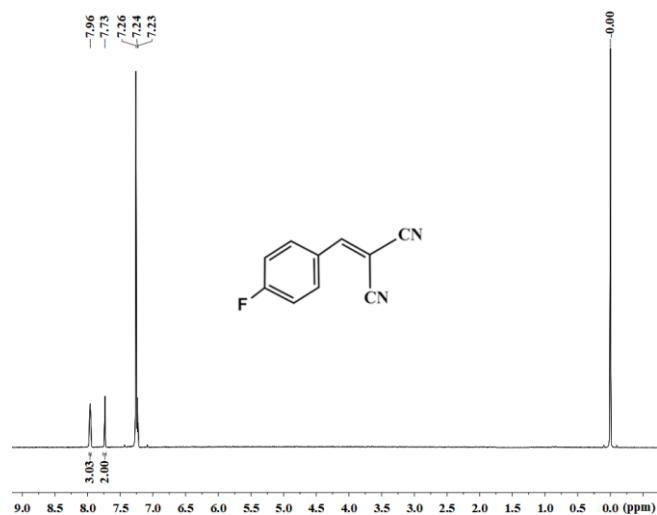


Figure S26. ^1H NMR spectrum of 2-(4-fluorobenzylidene)malononitrile in CDCl_3 .

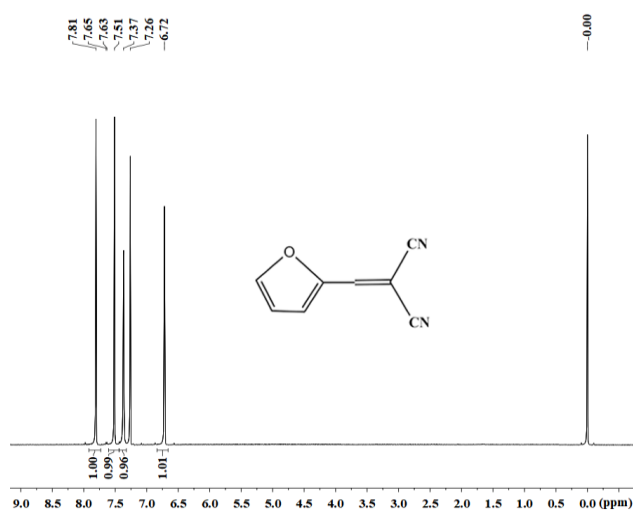


Figure S27. ^1H NMR spectrum of 2-(furan-2-ylmethylene)malononitrile in CDCl_3 .

References

- 1 Y. Zhang, Y. Zhang, C. Wang, X. Liu, Y. Fang, Y. Feng, *Green Chem.*, 2016, 18, 392-396.
- 2 S. Li, S. Zhao, *Analytica Chimica Acta*, 2004, 501, 99-102.
- 3 M. Idouhar, A. Tazerouti, *J Surfact Deterg*, 2008, 11, 263-267.